BIOLOGICAL SCIENCES: Neuroscience

The ventral aspect of the visual form pathway is not critical for the perception of biological motion

Short title: Ventral stream and biological motion perception

Gilaie-Dotan S[1,2,*], Saygin AP[3], Lorenzi L[4], Rees G[1,2] & Behrmann M[4]

1 Institute of Cognitive Neuroscience, University College London, London, WC1N 3AR, UK

2 Wellcome Trust Centre for Neuroimaging, University College London, London, WC1N 3BG, UK

3 Department of Cognitive Science and Neurosciences Program, University of California San Diego, San Diego, California, 92093-0515, USA

4 Department of Psychology, Carnegie Mellon University, Pittsburgh, Pennsylvania, 15213 USA

***Corresponding author:**

Sharon Gilaie-Dotan, Institute of Cognitive Neuroscience, Alexandra House, 17 Queen Square, London WC1N 3AR, UK, Tel: +44-20-7679-1122, Fax: +44-20-7813-2835. E-mail: shagido@gmail.com, s.gilaie-dotan@ucl.a.uk

Keywords: ventral stream, visual form agnosia, action, point light displays, motion pathway, FBA, EBA, brain damage, movement

ABSTRACT

Identifying the movements of those around us is fundamental for many daily activities such as recognizing actions, detecting predators, and socially interacting with others. A key question concerns the neurobiological substrates underlying biological motion perception. While the ventral "form" visual cortex is consistently activated by biologically moving stimuli, whether these activations are functionally critical for biological motion perception or are epiphenomenal remains unknown. To address this we examined whether focal damage to regions of ventral visual cortex causing significant deficits in form perception adversely affects biological motion perception. Six patients with damage to ventral cortex were tested with sensitive point-light display paradigms. All patients were able to recognize unmasked point light displays and their perceptual thresholds were not significantly different from those of three different control groups, one of which comprised brain-damaged patients with spared ventral cortex (n>50). Importantly, these six patients performed significantly better than patients with damage to regions critical for biological motion perception. To assess the necessary contribution of different regions in the ventral pathway to biological motion perception, we complement the behavioural findings with a fine-grained comparison between the lesion location and extent and cortical regions standardly implicated in biological motion processing. This analysis revealed that the ventral aspects of the form pathway (e.g. fusiform regions, ventral EBA) are not critical for biological motion perception. We hypothesize that the role of these ventral regions is to provide enhanced multi-view/posture representation of the moving person rather than to represent biological motion perception per se.

SIGNIFICANCE STATEMENT

Perceiving the movements of people around us is critical for many daily skills (from detecting threats to social interactions) and involves both form and motion perception. Even though the “form” visual pathway is consistently activated in response to biological motion stimuli, it is unknown whether this pathway’s integrity is critical for perceiving biological motion. Here, we examined whether damage to different aspects of the form pathway affects biological motion perception. Individuals with lesions to the ventral aspects of this pathway evinced normal biological motion perception despite their impairments in form perception. Our counterintuitive findings indicate that biological motion can be perceived and processed normally even when the ability to perceive the form or the actor executing the movements is impaired.

INTRODUCTION

Perception of the movements of other peoples' bodies is fundamental to human survival and daily interactions (e.g. motor learning, social interactions, anticipating actions of others), and is sufficiently robust so as to succeed even under suboptimal conditions (e.g., poor illumination and even partial occlusion (1-6)). A clear demonstration of the strength of this ability is the ease with which people recognize biological motion from point-light displays (PLDs) that consist of only a small set of moving points that mark joints on the body (7), Fig. 1A, left panels). These stimuli appear to naïve observers as a set of incoherent dots when static, but evoke a vivid percept of a moving person when in motion. Observers are able to infer movement information such as the motion or direction of the figure in these impoverished PLDs even under conditions of masking, added noise (8-11), or night driving (3, 4, 12).

Examination of the neural correlates of the perception of body movement reveals a widespread cortical network (13). Because biological motion perception, in natural vision or in PLDs, involves both form and motion perception (14), unsurprisingly, cortical regions associated with form and motion perception are activated. It is unclear, however, whether all of these brain areas contribute causally to the perception of biological motion. Neuropsychological studies in patients and TMS studies in normal observers have identified several motion-sensitive areas as critical for biological motion perception, including the pSTS and ventral premotor cortex (vPMC, (11, 15-17)), given that a sustained or transient lesion to these regions impairs biological motion perception. However, whether form-sensitive regions in the ventral "form" visual pathway (for example, the extrastriate body area (EBA (18-20) in the lateral occipital cortex), that are consistently activated in response to biological

motion in neuroimaging studies, play a critical role in biological motion perception remains unknown.

PLDs constitute ideal stimuli with which to explore whether the engagement of ventral visual cortex is necessary in biological motion perception, as these displays permit the presentation of recognizable body movements whilst dissociating them from "classical ventral" form cues such as contour, surface, shape, texture and color. As such, PLDs are thought to depict dynamic body and action information solely via *motion* cues. To the extent that the ventral form pathway is involved in PLD perception, this cannot be attributed to processing "classical ventral" form cues. Even in the absence of classical form cues, however, moving PLDs convey coarse form information of the dynamic body and investigating the structure of the articulated body that can be retrieved from the coherent movement of the dots has been a central driving motivation in biological motion research (e.g. (21-27)). This has been true since the pioneering work of Johansson (7), and therefore, unsurprisingly, these displays have often been termed biological structure-from-motion or form-from-motion. Whether the processes supporting biological motion perception, in the absence of classical form cues, critically depend on the form computations of the form visual pathway still remains unknown (20, 28-30).

One way to address this issue is to study how damage to the ventral "form" visual pathway affects the perception of biological motion. Our predictions are straightforward: if ventral stream integrity and ventral form-representations are necessary for the perception of biological motion, then individuals with form perception deficits following damage to ventral visual cortex (including damage to specific areas implicated in biological motion processing and/or areas implicated in

body form perception (e.g. the EBA (18-20)), should be impaired at perceiving biological motion.

To test this hypothesis, we tested a group of six patients with form perception deficits following a circumscribed lesion to ventral visual cortex in adulthood (see Table 1). Using PLDs and paradigms that are successful in detecting biological motion perceptual deficits following brain damage (11, 17), we measured the patients' recognition and perception of biological motion in two different experiments. We compared each patient's performance to that of three different control groups: a brain-damaged control group of 54 patients whose cortical lesions fell outside of the ventral visual cortex, a group of healthy age-matched controls (patient-specific), and a group of 13 young control participants. The importance of the brain-damaged control group is twofold. First, comparing the ventral patients to patients with non-ventral lesions allowed us to determine whether biological motion perception, if affected, is specifically a consequence of a ventral lesion or of brain damage, more generally. Second, because a subset of patients in the non-ventral control group have lesions to brain areas known to significantly impair biological motion perception (pSTS and vPMC), we can compare directly the perceptual thresholds of the ventral patients with those of individuals with identified deficits in biological motion following damage to pSTS or vPMC. Finally, given that ventral cortex constitutes a large swath of cortex and that patients' lesions were not identical, we assessed the brain-behavior correspondences further by examining, at a finer grain, which, if any, affected subareas affect biological motion perception. To do so, for each patient, we carefully delineated the lesion, assessed the magnitude of the damage, and situated the lesion relative to regions in ventral, lateral and middle temporal cortex that are standardly

associated with biological motion processing, including body parts and visual motion sensitive regions (e.g. (13, 20, 31-34)).

To anticipate our findings, we show that biological motion recognition and perceptual thresholds of the ventral patients consistently fall within the normal range of all three control groups. Thus, our results indicate that the perception of biological motion (i) does not depend on the integrity of the ventral aspects of the form (ventral) visual pathway or the integrity of the ventral portion of the EBA (ventral to hMT/V5), and (ii) can be dissociated from form perception. In light of the above, we hypothesize that computations that suffice for the perception of biological motion are mediated by mechanisms independent of the "form" ventral cortex, and that such computations may be based on motion cues that represent movement kinematics rather than on form information per se.

RESULTS

Experiment 1: Recognition and perceptual thresholds for biological motion

At the start of Experiment 1, participants were presented with unmasked PLDs (see Figure 1A, left panels) and were asked to describe what they perceived. For these unmasked PLDs, all six ventral patients (as well as almost all individuals in three groups of controls) were able to name the movements effortlessly and immediately, even without prior knowledge of or training on PLDs. This observation is consistent with previous work (35-39), showing that patients are generally able to recognize unmasked PLDs of biological motion (40). Only two of the control patients with brain-damaged outside of ventral cortex (from the 'brain-damaged control group' in the current study) were unable to recognize unmasked PLDs (11).

After this recognition phase, perceptual thresholds for biological motion (number of noise points at which performance is 82% accurate, see Figure 1A right panel for illustration) were measured for all participants (Figure 1B and detailed in Table 2). Consistent with previous results showing that the perceptual thresholds of brain-damaged patients for biological motion are significantly lower than those of healthy age-matched controls (11), four of the ventral visual patients' (CR, SM, EC, and SH) perceptual thresholds were at the lower end of their matched controls' distribution (control group 1, light diamonds in Figure 1B), but *not statistically different* (see Table 2 for statistical details). Moreover, the perceptual threshold of each ventral patients was also *within the norm* of the younger control group (control group 2; all $|t_{(12)}|$'s < 1.44, all p's > 0.17 (41), see Figure 1B, light gray circles).

We then compared the thresholds of the ventral patients and those of 54 patients with unilateral non-ventral brain damage (control group 3 (11), dark circles in Figure 1B). If the integrity of the ventral visual cortex is critical for biological motion perception, then the performance of the ventral visual patients should be significantly poorer than that of patients with brain damage elsewhere. In contrast, the ventral patients' thresholds were trending to be significantly better than their brain-damaged controls (Wilcoxon non-parametric rank-sum test: ventral patients (median=13.11, n=6) vs. brain damaged controls (median=9.82, n=54): U = 258, p = 0.06). Also, in an individual case analysis, each of the ventral visual patients' performance was better than the average performance of the right only (n=11), left only (n=43) or combined right and left hemisphere brain-damaged control patients (see Table 2 for full details). All of these comparisons indicate that the six ventral patients performed well within the range of other (non-ventral) brain-damaged patients, thereby ruling out a specific role for ventral cortex in biological motion perception.

The data from the control brain-damaged patients were taken from a previous study (11) that revealed that lesions to left posterior STS (L-pSTS) or to left ventral premotor cortex (L-vPMC) had the greatest adverse effect on biological motion perception. The function and structure of these regions are associated with biological motion perception (11, 15, 16, 20, 42-46) and their role in biological motion perception has been confirmed in several TMS studies (15, 16). In light of this, these data permit a stringent comparison between the performance of our ventral patients and that of the brain-damaged patients with lesions to L-pSTS or L-vPMC (the two "critical" lesion groups). As shown in Fig. 1C, the ventral visual patient group performed significantly better (had higher perceptual thresholds, meaning they could tolerate more noise points) than both of the "critical" lesion groups (Wilcoxon non-parametric rank-sum test: ventral patients (median=13.11, n=6) vs. lesioned L-pSTS (median=7.1, n=9): $U = 73$, $p = 0.0016$; ventral patients vs. lesioned L-vPMC (median=7.6, n=10): $U = 77$, $p = 0.003$). Furthermore, in single-case comparisons (each ventral patient vs. the critical control groups (41)), four of the ventral visual patients performed significantly better than the critical control groups (see Table 2 for details). These results indicate that damage to ventral visual cortex, unlike damage to pSTS or vPMC, does not impair biological motion perception.

Experiment 1: Response times for biological motion

The results thus far indicate that biological motion perception does not rely on ventral stream integrity. To confirm this and ensure that the results were not a product of a speed-accuracy tradeoff, we examined RTs even though participants were informed that speeded responses were not required and were allowed to speak and take breaks (see Figure 1D). The responses of the patients were not significantly

slower than their age-matched controls (Wilcoxon non-parametric rank-sum test: ventral patients (median=7.78s, n=6) vs. age-matched controls (median=5.21s, n=33): U = 159, p = 0.134, z=1.5. This also held true for five ventral patients under single-case comparisons of patient vs. age-matched control group (2-tailed, |t|'s < 0.5, p's > 0.63 (41)). EC was significantly slower than her age-matched controls (t(11) = 4.74, p = 0.0008); however, this is almost certainly a result of the fact that she spoke during the experiment, even after being reminded to withhold comment. These results confirm that RTs were within the normal range for the ventral patients and that the normal perceptual thresholds did not result from elongated response times.

Experiment 2: Recognition and perceptual thresholds for biological motion under a different paradigm

To provide additional support for the findings from Experiment 1, we further examined the perceptual thresholds of the ventral patients using a modified biological motion experimental paradigm. This task included a larger set of biological motion animations, different presentation and task requirements, and provided feedback. In this experiment, each trial consisted of one centrally displayed PLD (see Figure 2A) observers determined whether there was a moving human figure embedded in the display (compare Fig 2A middle and right panels, see Methods). During the action recognition phase (Fig. 2A left panel), all ventral patients and their controls effortlessly reported the actions present in the PLDs. Moreover, the ventral patients' perceptual thresholds fell within the normal range of their age-matched controls (see Fig. 2B; CR: t(14)=-1.42, p>0.17, SM: t(14)=-0.88, p>0.39, EC: t(14)=-0.76, p>0.45,

EL[1]: t(10)=0.30, p>0.77, GB[1]: t(10)=1.55, p>0.15, SH[1]: t(10)=-0.65, p>0.53). Of great interest, the perceptual thresholds established here for each of the patients (and the relative rank ordering of the patients) were very similar to those obtained in Exp. 1, reflecting the reliability and consistency of these measures.

Experiment 2: Response times for biological motion under a different paradigm

The analysis of the RTs of the patients versus the age-matched controls revealed no significant group differences (see Figure 2C; all patients but EL: |t|'s <0.79, p's >0.45, EL: t(10) = 1.51, p>0.16), again confirming that the patients performed within the normal range.

Subjective reports about biological motion perception

As a converging source of evidence, we obtained self-reports from the patients and controls in response to questions such as whether, on the basis of gait, they were able to recognize individuals and discriminate the age and gender of an individual, and, for the patients, whether these abilities have changed post-injury. All patients as well as controls reported that they can comprehend movement patterns and actions even when they cannot recognize the person doing it. They also reported that they can discriminate gender and age based on gait, and that they can easily recognize atypical gait (e.g. limping). None of the patients reported that their abilities changed following their brain injury. Although these reports are subjective, they provide additional indications that biological motion perception may be dissociable from form perception.

[1] The performance of EL, GB and SH also fell in the normal range of a bigger control group n=14, aged 6-.2+/-6.45 (SD)): |t(13)|'s > 0.5, p's > 0.6.

Relationship of perceptual performance to underlying lesion

The experimental findings reveal that the six ventral patients performed as well as or even better than (see comparison against patients with frank pSTS or vPMC lesions) the various control groups. We have proposed that the dissociation between the form deficit and intact biological motion perception rules out the functional contribution of ventral cortex.

A possible alternative explanation, however, is that, because ventral cortex is so extensive and lesions are more circumscribed, there may be sparing of key ventral regions associated with biological motion processing (13) and it is these spared regions that account for the normal perceptual performance. To assess this possibility, first, we carefully delineated the lesion of each patient and transformed each lesion into normalized MNI space. Second, we superimposed the lesion onto ventral cortex in which we identified areas that are consistently activated by biological motion; this included regions responsive to the perception of body movement (blue in Figure 3), sensitive to static bodies (yellow in Figure 3), to human movements (green in Figure 3) as determined by a recent meta-analysis ((13), see Methods), as well as motion-sensitive hMT/V5, biological motion sensitive pSTS, vPMC, and static-body sensitive EBA (18-20). For the EBA cluster, we further distinguished between three subregions: the ventral portion (ventral and not overlapping hMT/V5), the portion overlapping hMT/V5, and the portion anterior to hMT/V5. Our analysis also took into consideration the functional anatomical organization of the ventral visual stream (e.g. ventral surface vs. lateral-occipito-temporal aspects). Third, for each of these regions, we evaluated the extent of damage in each patient. The results of this fine-grained analysis are detailed in Table 3.

Our analysis revealed that regions situated on the ventral surface (e.g. fusiform gyrus) that are assumed to be engaged in some aspect of biological motion perception are substantially damaged in three patients (60-100%, left regions in GB and SH, and the right regions in EC, see Table 3), including the regions that are sensitive to static body perception, body movements in general, and human body movements' selectivity (13). Furthermore, the ventral portion of the EBA (47, 48), situated ventrally to but not overlapping hMT/V5, is also critically damaged in two right ventral patients (SM and EC) and partially damaged in left ventral patient (GB). From these observations, we can conclude that regions situated on the ventral surface of the cortex in the ventral stream (20, 31, 49) and the ventral aspect of the EBA are not contributing critically to biological motion perception. Because other regions such as those on the lateral occipito-temporal surface, including hMT/V5 and other parts of EBA, are only partially damaged in some of the patients (20-60%), we cannot rule out their possible role in biological motion perception.

While each of the regions associated with biological motion in the ventral aspect of the cortex is significantly damaged in one or more of the patients (R-fusiform in EC, L-fusiform in GB and SH), including the right and left ventral portions of the EBA (R-vEBA in EC and SM, L-vEBA in GB), and also left MT+/V5 (EL), the superior and middle temporal regions are mostly spared (except for EL). Importantly, the two areas that are well-known to be sensitive and critical to human motion, pSTS and vPMC (11, 13, 16, 28, 30, 32, 46, 50), are spared in all cases.

Despite the fact that ventral regions associated with different aspects of biological motion processing were impacted by the lesions, the ventral patients performed as well as healthy controls and brain-damaged patients. Importantly, the ventral-lesioned

patients performed better than patients with brain damage to regions pSTS and vPMC, standardly considered the neural correlates of biological motion perception.

DISCUSSION

In this study, we explored whether the integrity of form perception and of ventral visual cortex are necessary for the perception of biological motion. This was achieved by examining the perceptual performance of patients with documented form deficits following brain damage to ventral visual cortex. In two studies using animated point light displays (PLDs, (7)) embedded in noise points, we derived a host of dependent measures (accuracy of unmasked displays, thresholds, RTs and self report measures) There were no differences between the patients' indices and those of matched controls or of brain-damaged patients with spared ventral cortex, and this was also true when compared with healthy young controls. Moreover, the patients performed significantly better than patients with documented damage to regions critical for biological motion (pSTS and vPMC (11)). Further, by showing that large swaths of cortex, assumed to be associated with biological motion perception, were lesioned in these patients, we were able to determine that the integrity of the ventral aspects of the ventral visual pathway is not critical for normal biological motion perception.

The role of the ventral visual pathway in biological motion processing

Ventral and occipito-temporal regions, which comprise ventral visual cortex, are associated with the processing of form information ("form pathway"). Perhaps surprisingly, these very regions, including the extrastriate body area (EBA), are activated in neuroimaging studies that focus on biological motion ((13, 19, 30, 51), see Figure 3 and 4). A possible explanation for the engagement of these areas in

biological motion processing is that form-based computations may be implicated in biological motion processing (7, 21-25). Indeed, some have suggested that PLDs might be better characterized as “motion-from-form” (26), and recent models of biological motion recognition have proposed that biological motion recognition computations can be based on a sequence of static form snapshots derived from the movement itself ((52, 53), Figure 4A). Some support for this comes from physiological recordings in non-human primates, where biological motion sensitive neurons show sensitivity to body form in addition to or instead of body motion (54-56).

The key question is whether the engagement of these cortical ventral areas is functionally relevant for the perception of biological motion. The answer cannot be reached based on findings from functional imaging and thus, determining causality remains elusive. Our results indicate that intact ventral regions in the form visual pathway (e.g. along the fusiform gyrus) are not necessary for biological motion perception. Why are these areas activated then as revealed in neuroimaging investigations? One possibility is that following damage to ventral visual cortex, cortical function is reorganized such that other regions become critical for biological motion perception. However, notably, all our patients performed within the normal range of other, non-brain-damaged control participants thus indicating that if any such adaptive plasticity occurs, it is surprisingly effective. An alternative possibility we propose is that these ventral regions play a role in the representation of the actor and his/her identity and, hence, are activated during biological motion processing. Specifically, a series of static posture snapshots may suffice for a whole-body viewpoint-based representation of the actor (Figure 4A). Thus, while actor recognition and the form executing the motion may be computed by the ventral form pathway, the

motion kinematics themselves, may be computed the motion pathway (Figure 4A). When the ventral aspects of the ventral visual cortex are damaged (an example is conveyed in Fig. 4A by red colored markings based on our ventral visual patients), snapshots leading to *actor* recognition might be disrupted. However, because the computations of kinematics mediated by the motion pathway are not significantly affected, *movement* perception is unaffected. Figure 4B illustrates the prediction of this model for PLDs to illustrate our current findings. In addition to the supporting evidence from our patients and even from individuals with developmental agnosia (57, 58), form-based and motion-based processing of body motion can be dissociated among healthy controls (59).

Parallel processing routes supporting biological motion perception?

The notion that biological motion perception might be computed in more than one way is also compatible with findings from a series of neuropsychological case studies. For example, LM, the "motion blind" patient with lesioned MT+/V5 (37), and AF with severe damage to dorsal cortex (36) are both able to recognize unmasked point light displays above chance. In addition, patients with brain damage or abnormal vision such as patient MM (38), who recovered from long term visual deprivation, or patient JW who has widespread occipital damage following hypoxia (60), are both able to successfully recognize unmasked point light displays. Finally, the above-chance biological motion performance of patients with lesions that appear to invade early visual areas (36, 61) and are very different from the lesions of the patients examined in our current study, also seems to suggest multiple processing routes supporting biological motion perception.

Although all of these findings, along with the present results, are consistent with an account in which biological motion perception may be achieved via multiple pathways, there is still some selectivity to the processing, and there are indications that biological motion perception is independent from other lower-level motion perception. For example, performance in biological motion and motion coherence tasks are not correlated, as revealed in studies of patients (11), following congenital cataract (62), or healthy controls (44). Indeed, all our ventral patients performed normally in the biological motion tasks but some have basic motion perception deficits (SM, CR, and EC are impaired in motion coherence and motion detection tasks (63)). Similarly, patients AF and LM perform poorly on early motion tasks despite above chance performance on biological motion (36, 37).

If biological motion recognition can be achieved via multiple pathways, this duplication might reflect the importance of this process to a multiplicity of abilities, such as social communication, motor learning, and theory of mind. Whether these pathways achieve movement recognition independently remains to be resolved. What is certain, though, is that the integrity of the ventral aspects of the ventral visual stream is not in and of itself critical for the normal perception of biological motion.

CONCLUSIONS

We have shown that biological motion perception can be achieved in spite of damage to the ventral aspect of the form visual pathway (e.g. FBA, v-EBA). While regions such as pSTS and vPMC are critical for biological motion perception (11, 15, 16, 42, 64, 65), we speculate that the ventral regions of the form visual pathway are critical for recognizing the person performing the movement, but not for recognizing the motion being performed.

METHODS

Patients with ventral visual lesions

Six premorbidly normal right-handed individuals who sustained brain damage to the right (n=2), left (n=3), or bilateral (n=1) ventral visual cortex participated in the study. Following a lesion sustained in adulthood (except for CR who was aged 16 years), all individuals reported visual perceptual problems and have well-established form processing deficits. Table 1 summarizes the key demographics, neuropsychological descriptions, and detailed visual performance (including visual motion perception) of each patient; further details are available in Supplementary Material and in earlier publications (SM (63, 66-72), CR (63, 67-69, 72), EL (63, 72-77), GB (63, 77), SH (72, 77) and EC (63)).

Experiment 1

In this experiment, we used unmasked point-light displays (PLDs) to assess recognition of biological motion, and then measured perceptual thresholds using PLDs masked in noise points. To assess recognition of biological motion, unmasked point light display animations of actions (see below) were presented and participants were required to verbally describe the stimuli without having prior knowledge of what these would be. Each point light animation looped until a coherent verbal description was given, after which the experimenter presented the next animation. To measure perceptual thresholds, on each trial, two point-light displays were presented simultaneously on the right and left sides of the screen, one containing a moving upright human figure performing one of seven actions (see Stimuli below, Figure 1A,

Supplementary Material and Supplementary Figures S1-S3 (11, 57, 78)), and the other a spatially scrambled version of the same action. The side of the biological motion animation was randomly determined on each trial. Participants were instructed to identify which of the two displays contained the animation of the human movement (but did not have to identify the movement i.e., jogging or walking, except in the action recognition phase, see below). Both animations (intact and scrambled movements) were embedded in a number of noise points adaptively determined according to the participant's performance (79). The task became more difficult as the number of noise points increased. Perceptual thresholds were determined based on the number of noise points with which a participant could perform at a predefined level of accuracy (82%). Stimuli and further procedures are fully described in Supplementary Material and elsewhere (11, 57).

Participants

All six ventral-lesion patients, tested in Pittsburgh, and all healthy control participants (tested in Pittsburgh or in London) gave written informed consent to participate in the study and the experiments were approved by local ethics committees (Institutional Review Board, Carnegie Mellon University and UCL). All patients (except SM who was tested at CMU) and the older controls were tested at home for maximal convenience.

Procedures regarding the data collection from the non-ventral brain-damaged patient control group (control group 3, see below) are provided elsewhere (11). Informed consent was obtained from these patients at the time of testing in accordance with guidelines of the UCSD and VA Northern California Health Care System Human Research Protections Programs. The findings from these patients have

been published previously (11) and we simply adopted the de-identified data to serve as an additional benchmark against which to compare the ventral patients' performance.

Healthy controls

All healthy control participants had normal or corrected-to-normal vision, no history of neurological disorders, and were right-handed.

Control group 1. The first neurologically-normal control group that participated in this study included 42 healthy adults, age-matched to the patients: 16 male control participants served as age-matched controls for CR (mean age 32.0 years ± 2.9 (S.D.)), 15 males served as age-matched controls for SM (mean age 35.2 years ± 3.3 (S.D.), 11 of whom were also matched for CR), 13 females and one male (matched for SM as well) served as age-matched controls for EC (mean age 48.0 years ± 3.8 (S.D.)), and 14 females and one male served as age-matched controls for GB, EL, and SH (aged 50-70, mean 59.2 ± 6.1 (S.D.), of whom 5 females were matched for EC as well).

Control group 2. The second neurologically normal control group included 13 healthy young controls (aged 20.4 ± 1.08 (S.D.)).

Brain-damaged controls

Control group 3. The third control group included 54 right-handed, brain-damaged patients (13 females, 41 males, aged 36.9 – 84.9 years) with focal, unilateral lesions (43 in the left hemisphere, 11 in the right hemisphere). From among the group of 60 patients who had completed Experiment 1 in an earlier study (11), we selected for this control group only those for whom we could definitively determine that their

ventral visual cortex was not affected by their lesion (as ascertained and confirmed by the lesion boundaries) as determined from computerized lesion reconstructions of the brain. The time between testing and patients' cerebrovascular accident (CVA) ranged from 6 months to 22 years (mean of 6.5 years). Patients with diagnosed or suspected vision or hearing loss, dementia, head trauma, tumours, multiple infarcts or prior psychiatric or neurological abnormalities were excluded from the sample. Motor and language impairments ranged from very mild to severe in the sample, but all patients were able to understand and carry out the task. None of the patients presented with spatial neglect or other attentional disorders.

Stimuli

Briefly, biological motion animations made of 12 white points on a black background depicting one of seven actions: (walking, jogging, overarm throwing, underarm throwing (bowling), stepping up, high kicking into the air, and lower kicking) and lasting 0.8 s were presented, and looped until a response was given. For the perceptual threshold assessment, a matched spatially-scrambled version was created for each animation so that the local motion of each point was preserved, without the global form (11, 57, 78).

In each trial of the perceptual threshold assessment, additional moving noise points were randomly superimposed on both PLDs (the biological motion and its scrambled counterpart, (9)). The motion trajectory of each noise point that was added to the animations was equivalent to a motion trajectory of one of the animation's points (randomly chosen), but starting at a random location.

Each animation subtended approximately 4x6 degrees (width x height) visual angle when viewed from 55 cm. The total area occupied by each PLD (comprising the

animation plus the noise points) was approximately 7 degrees of visual angle in diameter. The two point-light displays (biological motion and its scrambled counterpart) were displayed at approximately 9 degrees to the left and right of the centre of the screen, their vertical centers horizontally aligned (see Supplementary Figure S1). Stimuli were presented and responses recorded using MATLAB (Mathworks, Natick, MA, USA) and the Psychophysics Toolbox V2.54 (80, 81).

Procedure

In the first part of the experiment, we examined action recognition of unmasked point light displays. Participants were presented with seven different unmasked biological motion animations and were asked to verbally describe the stimuli on the screen. Each animation was displayed separately in the centre of the screen without any masking noise points and looped until the verbal description given by the participant indicated that they were able to perceive the movement conveyed by the point light animation. After that, the experimenter displayed the next animation.

Following the action recognition phase, sensitivity to biological motion was assessed by measuring the number of noise dots that allowed successful discrimination (82%) of intact from scrambled animations when both are masked in noise points. On each trial, participants were required to report whether the intact PLD ("the person") was on the right or left side of the screen by pressing the corresponding left or right key in a 2AFC manner (see additional details below). The animations looped until a response was given. Although accuracy was the key dependent measure, response time of each trial was also recorded. EC, EL, the brain-damaged controls, and some of the older healthy controls replied verbally or by pointing, after which the experimenter pressed the corresponding response button.

Since the PLDs were presented on the two sides of the screen simultaneously, participants were not required to fixate at the centre of the screen. After 16 practice trials with a predefined number of noise points, control participants completed 118 trials presented in two blocks separated by an optional rest period, while patients completed one block of 73 trials, with a rest period after 40 trials. Note that because the task was not timed, participants were able to take additional breaks at any time if needed.

To estimate perceptual thresholds, we varied the number of noise points in each trial to yield a psychometric measure of performance according to an efficient Bayesian adaptive procedure that uses the mean of the posterior probability density function (QUEST, (79)). The perceptual threshold was determined as the number of points at which a participant performed at 82% accuracy. For the healthy controls, who performed two blocks of trials, thresholds from the two blocks were averaged.

Reaction times (RT) analysis was based on each participant's average reaction time across the experiment.

In addition to between-group comparisons, which were based on Wilcoxon non-parametric rank-sum test (82), we also examined every patient's performance individually. This was achieved by determining whether a patient's performance (threshold or RT) was significantly different from that of a control group. The statistical evaluation was based on an established statistical procedure for comparing single cases to a control group (41) entailing a modified t-test, significant performance differences roughly corresponding to more than two standard deviations from the controls' mean performance.

Experiment 2

The previous experiment assessed the participant's ability to detect the PLD containing human movement when embedded in noise. This second experiment further examined the patients' biological motion perception using a slightly different method including a different and larger set of displays and a different criterion at which threshold is established. We first assessed action recognition of 12 different PLDs (see Supp. Mat.). Participants were asked to describe what they perceived so as to ensure that they were able to recognize the movements conveyed by PLDs. Thereafter, perceptual thresholds were established. A short practice comprising a few trials with a predefined number of noise points was completed, followed by the main experiment that measured the number of noise points a participant can tolerate and perform at 75% accuracy, using the same Bayesian estimation method as in Experiment 1 (79). In each trial, a single PLD (similar to those from Experiment 1, see Figure 2A and Supp. Mat.) was presented at the center of the screen, either containing a movement of an upright human figure performing a movement (target), or a spatially scrambled version of it (non-target). Animations (targets and non-targets) were masked in noise points (in the same manner as in Experiment 1), and the participant's task was to decide whether the display contained a person ('target present') or not ('target absent') in a 2AFC manner using two predefined keys. Animations looped until a response was given. Visual feedback (green/red cross for correct/incorrect response) was provided after each response. As in Experiment 1, speeded responses were not required but we still recorded response times. Further experimental details are similar to those of Experiment 1; see details in Supplementary Material.

Participants

All six ventral-damaged patients, tested in Pittsburgh, and 39 healthy neurologically normal controls (28 also participated in Experiment 1) gave informed consent to participate in the study and the experiment was approved by local ethics committees (see Experiment 1). The controls were age-matched to each patient in the following way: 15 control participants (14 male) served as age-matched controls for CR (mean age 32.5 years ± 4.1 (S.D.)), 15 control participants (12 male) served as age-matched controls for SM (mean age 37.3 years ± 4.5, 10 of whom were also matched for CR), 15 controls (12 female) served as age-matched controls for EC (mean age 46.5 years ± 4.5, 5(1) controls also matched for SM (CR)), and 11 controls (8 females) served as age-matched controls for GB, EL, and SH (mean 62.7 ± 4.6, 1 also matched for EC). All patients (but SM who was tested at CMU) and some of the controls were tested at home for maximal convenience.

Lesion and anatomical analysis

Lesion delineation procedure

For structural image acquisition details see Supplementary Material. We used a lesion delineation procedure that has been successfully employed previously (63). For patients with high-resolution anatomical images (EL, SM, and CR), the images were coregistered onto a T1 MNI canonical SPM image using SPM (http://www.fil.ion.ucl.ac.uk/spm), after which their lesions were traced manually in MRIcroN (http://www.cabiatl.com/mricro/mricro, see Supplementary Material for tracing criteria) and saved as a binary image. For each patient, the co-registered

anatomical images and the demarcated lesion were normalized into MNI space using the unified normalization segmentation of SPM (http://www.fil.ion.ucl.ac.uk/spm).

For GB, EC, and SH, who had low-resolution anatomical images from their clinical scans, the lesion was traced manually onto the corresponding anatomical locations in an MNI canonical SPM image. To provide a consistent visualization of these patients' lesions (Figure 3), and to reach some approximate assessment of their lesion size (presented in Table 3), their non-continuous traced lesions were then each manually interpolated to a continuous lesion in a conservative manner using MRIcroN software. More details are provided in Supplementary Material.

Comparing lesions to regions associated with biological motion processing

To examine the lesion-behaviour relationships, we sited each of our patients' lesions relative to the anatomical locations of regions that are consistently activated in response to biological motion stimuli, as determined by a recent meta-analysis (13). Specifically, we were interested in regions that are consistently activated in response to (1) body movements (as reported in Grosbras et al. in Table 4 and Figure 1), to (2) static bodies (as reported in that study in Table 7 and Figure 3), or to (3) human movements vs. non-human movements (as reported in that study in Table 8). Three image maps from that meta-analysis corresponding to these three contrasts-of-interest were included in our analysis. Each image map consisted of probability (p) values that corresponded to the activation likelihood estimation (ALE) values reported in that study. These maps represent for each specific voxel the probability that a study will report significant activation in that voxel (for example with respect to one of our contrasts-of-interest: regions in which significant activation to human movements vs. non-human movements). The maps (as described in that study) were thresholded at

Z=3.2 (corresponding to p<0.0005) and cluster size was 120 mm^3 (see more details in (13)).

For each ventral patient, the three contrasts-of-interest from the meta-analysis along with the normalized brain and delineated lesion were loaded onto MRIcroN in four different colors as presented in Figure 2 (lesion in red, body-movement regions (contrast 1) in blue, static-bodies regions (contrast 2) in yellow, and selective human movements (contrast 3) in green). We then carefully examined whether the lesion invaded or overlapped any of the regions from each of the three contrasts-of-interest, according to anatomical location as well (e.g. ventral surface vs. lateral occipito-temporal regions). See also Table 3.

ACKNOWLEDGEMENTS

This study was supported by the Royal Society Travel for Collaboration grant TG102269 (SGD and MB), by Marie-Curie fellowship 236021 (SGD), by National Science Foundation BCS0923763 and NIMH 54246 (MB), by the National Science Foundation BCS-CAREER-1151805 (APS), and by the Wellcome Trust (GR). We thank all the patients and their families for their enthusiastic and wonderful collaboration. We thank Nina Dronkers and the VA Northern California Health Care System for allowing re-analyses of patient data and MRI scans, Ryan Egan for help with the data collection, Marie-Helene Grosbras for assisting and providing us the image maps from her meta-analysis study about human movement perception (13), Christina Konen, Solmaz Shariat Torbaghan, and Sabine Kastner for assisting with the anatomical images of EL and SM, Tanja Kassuba and Sabine Kastner for providing the functional localization of SM's MT+/V5, Adam Greenberg for help

with CR's anatomical images, Kate Fissell for providing and assisting with the anatomical images of EC and GB, Maxim Hammer for neuroradiological support, Mohamed Seghier for help with the lesion delineation process, and John Pyles for comments and discussion.

REFERENCES

1. Billino J, Bremmer F, & Gegenfurtner KR (2008) Motion processing at low light levels: Differential effects on the perception of specific motion types. *J Vis* 8(3):14 11-10.
2. Wood JM, *et al.* (2011) Using biological motion to enhance the conspicuity of roadway workers. *Accid Anal Prev* 43(3):1036-1041.
3. Tyrrell RA, *et al.* (2009) Seeing pedestrians at night: visual clutter does not mask biological motion. *Accid Anal Prev* 41(3):506-512.
4. Balk SA, Tyrrell RA, Brooks JO, & Carpenter TL (2008) Highlighting human form and motion information enhances the conspicuity of pedestrians at night. *Perception* 37(8):1276-1284.
5. Owens DA, Antonoff RJ, & Francis EL (1994) Biological Motion and Nighttime Pedestrian Conspicuity. *Human Factors: The Journal of the Human Factors and Ergonomics Society* 36(4):718-732.
6. Neri P, Morrone MC, & Burr DC (1998) Seeing biological motion. *Nature* 395(6705):894-896.
7. Johansson G (1973) Visual perception of biological motion and a model for its analysis. *Percept Psychophys* 14:201-211.
8. Pinto J & Shiffrar M (1999) Subconfigurations of the human form in the perception of biological motion displays. *Acta Psychol (Amst)* 102(2-3):293-318.
9. Bertenthal B & Pinto J (1994) Global processing of biological motion. *Psychol Sci* 5(4):221-225.
10. Pavlova M, Staudt M, Sokolov A, Birbaumer N, & Krageloh-Mann I (2003) Perception and production of biological movement in patients with early periventricular brain lesions. *Brain* 126(Pt 3):692-701.
11. Saygin AP (2007) Superior temporal and premotor brain areas necessary for biological motion perception. *Brain* 130(Pt 9):2452-2461.
12. Wood JM, Tyrrell RA, & Carberry TP (2005) Limitations in drivers' ability to recognize pedestrians at night. *Human factors* 47(3):644-653.
13. Grosbras MH, Beaton S, & Eickhoff SB (2010) Brain regions involved in human movement perception: A quantitative voxel-based meta-analysis. *Hum Brain Mapp*.
14. Kourtzi Z, Krekelberg B, & van Wezel RJ (2008) Linking form and motion in the primate brain. *TRENDS COGN. SCI.* 12(6):230-236.

15. Grossman ED, Battelli L, & Pascual-Leone A (2005) Repetitive TMS over posterior STS disrupts perception of biological motion. *Vision Res* 45(22):2847-2853.
16. van Kemenade B, Muggleton N, Walsh V, & Saygin AP (2012) The Effects of TMS over STS and Premotor Cortex on the Perception of Biological Motion. *J Cogn Neurosci* 24(4):896–904.
17. Vaina LM & Gross CG (2004) Perceptual deficits in patients with impaired recognition of biological motion after temporal lobe lesions. *Proc Natl Acad Sci U S A* 101(48):16947-16951.
18. Downing PE, Jiang Y, Shuman M, & Kanwisher N (2001) A cortical area selective for visual processing of the human body. *Science* 293(5539):2470-2473.
19. Peelen MV & Downing PE (2007) The neural basis of visual body perception. *Nat. Rev. Neurosci.* 8(8):636-648.
20. Jastorff J & Orban GA (2009) Human functional magnetic resonance imaging reveals separation and integration of shape and motion cues in biological motion processing. *J Neurosci* 29(22):7315-7329.
21. Thompson JC, Clarke M, Stewart T, & Puce A (2005) Configural processing of biological motion in human superior temporal sulcus. *J Neurosci* 25(39):9059-9066.
22. Beintema JA & Lappe M (2002) Perception of biological motion without local image motion. *Proc Natl Acad Sci U S A* 99(8):5661-5663.
23. Lu H (2010) Structural processing in biological motion perception. *J Vis* 10(12):13.
24. Reid R, Brooks A, Blair D, & van der Zwan R (2009) Snap! Recognising implicit actions in static point-light displays. *Perception* 38(4):613-616.
25. Thirkettle M, Scott-Samuel NE, & Benton CP (2010) Form overshadows 'opponent motion' information in processing of biological motion from point light walker stimuli. *Vision Res* 50(1):118-126.
26. Lange J, Georg K, & Lappe M (2006) Visual perception of biological motion by form: a template-matching analysis. *J Vis* 6(8):836-849.
27. Troje NF (2008) Biological Motion Perception. *The Senses: A Comprehensive References.*, ed al. ABe (Elsevier, Oxford), pp 231-238.
28. Vaina LM, Solomon J, Chowdhury S, Sinha P, & Belliveau JW (2001) Functional neuroanatomy of biological motion perception in humans. *Proc Natl Acad Sci U S A* 98(20):11656-11661.
29. Beauchamp MS, Lee KE, Haxby JV, & Martin A (2002) Parallel visual motion processing streams for manipulable objects and human movements. *Neuron* 34(1):149-159.
30. Grossman ED & Blake R (2002) Brain Areas Active during Visual Perception of Biological Motion. *Neuron* 35(6):1167-1175.
31. Peelen MV, Wiggett AJ, & Downing PE (2006) Patterns of fMRI activity dissociate overlapping functional brain areas that respond to biological motion. *Neuron* 49(6):815-822.
32. Pyles JA, Garcia JO, Hoffman DD, & Grossman ED (2007) Visual perception and neural correlates of novel 'biological motion'. *Vision Res* 47(21):2786-2797.
33. Grossman ED, Jardine NL, & Pyles JA (2011) fMR-adaptation reveals invariant coding of biological motion on human STS. *Front Hum Neurosci* 5:12.

34. Kourtzi Z, Krekelberg B, & van Wezel RJA (2008) Linking form and motion in the primate brain. *TRENDS COGN. SCI.* 12(6):230-236.
35. Schenk T & Zihl J (1997) Visual motion perception after brain damage: II. Deficits in form-from-motion perception. *Neuropsychologia* 35(9):1299-1310.
36. Vaina LM, Lemay M, Bienfang DC, Choi AY, & Nakayama K (1990) Intact "biological motion" and "structure from motion" perception in a patient with impaired motion mechanisms: a case study. *Vis Neurosci* 5(4):353-369.
37. McLeod P, Dittrich W, Driver J, Perrett D, & Zihl J (1996) Preserved and impaired detection of structure from motion by a “motion blind” patient. *Visual Cognition* 3:363-391.
38. Fine I, *et al.* (2003) Long-term deprivation affects visual perception and cortex. *Nat Neurosci* 6(9):915-916.
39. Huberle E, Rupek P, Lappe M, & Karnath HO (2012) Perception of biological motion in visual agnosia. *Frontiers in behavioral neuroscience* 6:56.
40. James TW, Culham J, Humphrey GK, Milner AD, & Goodale MA (2003) Ventral occipital lesions impair object recognition but not object-directed grasping: an fMRI study. *Brain* 126(Pt 11):2463-2475.
41. Crawford JR & Howell DC (1998) Comparing an Individual's Test Score Against Norms Derived from Small Samples. *J Clin Exp Neuropsychol* 12(4):482–486.
42. Saygin AP, Wilson SM, Hagler DJ, Jr., Bates E, & Sereno MI (2004) Point-light biological motion perception activates human premotor cortex. *J Neurosci* 24(27):6181-6188.
43. Sereno MI, Saygin AP, & Hagler DJ, Jr. (2003) Retinotopy in parietal and temporal cortex. *Neuroimage* 19:S1523.
44. Gilaie-Dotan S, Kanai R, Bahrami B, Rees G, & Saygin AP (2013) Neuroanatomical correlates of biological motion detection. *Neuropsychologia* 51(3):457-463.
45. Grossman E, *et al.* (2000) Brain areas involved in perception of biological motion. *J Cogn Neurosci* 12(5):711-720.
46. Peuskens H, Vanrie J, Verfaillie K, & Orban GA (2005) Specificity of regions processing biological motion. *Eur J Neurosci* 21(10):2864-2875.
47. Weiner KS & Grill-Spector K (2011) Not one extrastriate body area: using anatomical landmarks, hMT+, and visual field maps to parcellate limb-selective activations in human lateral occipitotemporal cortex. *NeuroImage* 56(4):2183-2199.
48. Ferri S, Kolster H, Jastorff J, & Orban GA (2012) The overlap of the EBA and the MT/V5 cluster. *NeuroImage* 66C:412-425.
49. Schwarzlose RF, Baker CI, & Kanwisher N (2005) Separate face and body selectivity on the fusiform gyrus. *J Neurosci* 25(47):11055-11059.
50. Bonda E, Petrides M, Ostry D, & Evans A (1996) Specific involvement of human parietal systems and the amygdala in the perception of biological motion. *J Neurosci* 16(11):3737-3744.
51. Downing PE, Jiang Y, Shuman M, & Kanwisher N (2001) A cortical area selective for visual processing of the human body. *Science* 293(5539):2470-2473.
52. Giese MA & Poggio T (2003) Neural mechanisms for the recognition of biological movements. *Nat Rev Neurosci* 4(3):179-192.
53. Lange J & Lappe M (2006) A model of biological motion perception from configural form cues. *J Neurosci* 26(11):2894-2906.

54. Vangeneugden J, *et al.* (2011) Distinct mechanisms for coding of visual actions in macaque temporal cortex. *J Neurosci* 31(2):385-401.
55. Jellema T & Perrett DI (2003) Cells in monkey STS responsive to articulated body motions and consequent static posture: a case of implied motion? *Neuropsychologia* 41(13):1728-1737.
56. Singer JM & Sheinberg DL (2010) Temporal cortex neurons encode articulated actions as slow sequences of integrated poses. *J Neurosci* 30(8):3133-3145.
57. Gilaie-Dotan S, Bentin S, Harel M, Rees G, & Saygin AP (2011) Normal form from biological motion despite impaired ventral stream function. *Neuropsychologia* 49(5):1033-1043.
58. Gilaie-Dotan S, Perry A, Bonneh Y, Malach R, & Bentin S (2009) Seeing with profoundly deactivated mid-level visual areas: non-hierarchical functioning in the human visual cortex. *Cereb Cortex* 19(7):1687-1703.
59. Miller LE & Saygin AP (2013) Individual differences in the perception of biological motion: links to social cognition and motor imagery. *Cognition* 128(2):140-148.
60. Rosenthal O & Behrmann M (2006) Acquiring long-term representations of visual classes following extensive extrastriate damage. *Neuropsychologia* 44(5):799-815.
61. Huberle E, Rupek P, Lappe M, & Karnath HO (2009) Perception of global gestalt by temporal integration in simultanagnosia. *Eur J Neurosci* 29(1):197-204.
62. Hadad BS, Maurer D, & Lewis TL (2012) Sparing of sensitivity to biological motion but not of global motion after early visual deprivation. *Dev Sci* 15(4):474-481.
63. Gilaie-Dotan S, *et al.* (2013) The role of human ventral visual cortex in motion perception. *Brain* 136(Pt 9):2784-2798.
64. Pelphrey KA, *et al.* (2003) Brain activity evoked by the perception of human walking: controlling for meaningful coherent motion. *J Neurosci* 23(17):6819-6825.
65. Tai YF, Scherfler C, Brooks DJ, Sawamoto N, & Castiello U (2004) The human premotor cortex is 'mirror' only for biological actions. *Curr Biol* 14(2):117-120.
66. Behrmann M & Kimchi R (2003) What does visual agnosia tell us about perceptual organization and its relationship to object perception? *J Exp Psychol Hum Percept Perform* 29(1):19-42.
67. Marotta JJ, Genovese CR, & Behrmann M (2001) A functional MRI study of face recognition in patients with prosopagnosia. *Neuroreport* 12(8):1581-1587.
68. Gauthier I, Behrmann M, & Tarr MJ (1999) Can face recognition really be dissociated from object recognition? *J. Cogn. Neurosci.* 11(4):349-370.
69. Behrmann M & Williams P (2007) Impairments in part-whole representations of objects in two cases of integrative visual agnosia. *Cogn Neuropsychol* 24(7):701-730.
70. Nishimura M, Doyle J, Humphreys K, & Behrmann M (2010) Probing the face-space of individuals with prosopagnosia. *Neuropsychologia* 48(6):1828-1841.
71. Konen CS, Behrmann M, Nishimura M, & Kastner S (2011) The functional neuroanatomy of object agnosia: a case study. *Neuron* 71(1):49-60.

72. Behrmann M & Plaut DC (2014) Bilateral Hemispheric Processing of Words and Faces: Evidence from Word Impairments in Prosopagnosia and Face Impairments in Pure Alexia. *Cereb Cortex* 24(4):1102-1118.
73. McKeeff TJ & Behrmann M (2004) Pure alexia and covert reading: Evidence from Stroop tasks. *Cogn Neuropsychol* 21(2):443-458.
74. Mycroft RH, Behrmann M, & Kay J (2009) Visuoperceptual deficits in letter-by-letter reading? *Neuropsychologia* 47(7):1733-1744.
75. Montant M & Behrmann M (2001) Phonological activation in pure alexia. *Cogn Neuropsychol* 18(8):697-727.
76. Behrmann M, Nelson J, & Sekuler EB (1998) Visual complexity in letter-by-letter reading: "Pure" alexia is not pure. *Neuropsychologia* 36(11):1115-1132.
77. Habekost T, Petersen A, Behrmann M, & Starrfelt R (2014) From word superiority to word inferiority: Visual processing of letters and words in pure alexia. *Cogn Neuropsychol*:1-24.
78. Ahlstrom V, Blake R, & Ahlstrom U (1997) Perception of biological motion. *Perception* 26(12):1539-1548.
79. Watson AB & Pelli DG (1983) QUEST: a Bayesian adaptive psychometric method. *Percept Psychophys* 33(2):113-120.
80. Brainard DH (1997) The Psychophysics Toolbox. *Spat Vis* 10(4):433-436.
81. Pelli DG (1997) The VideoToolbox software for visual psychophysics: transforming numbers into movies. *Spat Vis* 10(4):437-442.
82. Wilcoxon F (1945) Individual Comparisons by Ranking Methods. *Biometrics Bulletin* 1:80–83.
83. Kolster H, Peeters R, & Orban GA (2010) The Retinotopic Organization of the Human Middle Temporal Area MT/V5 and Its Cortical Neighbors. *Journal of Neuroscience* 30(29):9801-9820.
84. Allen JS, *et al.* (2008) Effects of spatial transformation on regional brain volume estimates. *NeuroImage* 42(2):535-547.

TABLES

Table 1

A summary of the visual perceptual functions and impairments of the six ventral patients. Most of these data have been reported earlier (see reference numbers adjacent to patient initials). We summarize the patients' abilities by noting the number of SDs each score deviates from the controls' mean.

	EL (63, 72-77)	GB (63, 77)	SH (72, 77)	CR (63, 67-69, 72)	SM (63, 66-71)	EC (63)
Lesioned hemisphere	Left	Left	Left	Right (+ left)	Right	Right
Age (gender)	61(F)	70(F)	69(M)	31(M)	37(M)	48(F)
Time from injury	15 years	3 years	6 years	15 years	19 years	8 years
Visual acuity[63]	Corrected to normal	Corrected to normal	Corrected to normal	Normal	Normal	Normal
Accommodation / convergence deficit[63]	None apparent or reported	None apparent or reported	None apparent or reported	None apparent or reported	None apparent or reported	None apparent or reported
Visual field deficits[63]	**Upper right visual field quadranta-nopia**	**Upper right visual field quadranta-nopia**	**Right homo-nymous hemianopia (largely resolved)**	Full visual field	Full visual field	Full visual field
Object perception	**Mild impairment (1-2 SDs)**	**Mild impairment (1-2 SDs)**	**Mild impairment (1-2 SDs)**	**Agnosic (3 SDs)**	**Agnosic (3 SDs)**	**Object recognition difficulties (screening)**
Face perception	**Mild impairment (1-2 SDs)**	**Mild impairment (1-2 SDs)**	**Mild impairment (1-2 SDs)**	**Proso-pagnosic (3 SDs)**	**Proso-pagnosic (3 SDs)**	**Face recognition difficulties (screening)**
Word perception	**Pure alexic (3 SDs)**	**Pure alexic (3 SDs)**	**Pure alexic (3 SDs)**	**Mild impairment (1-2 SDs)**	**Mild impairment (1-2 SDs)**	UNKNOWN
Motion perception – basic (detection)[63]	Normal	Normal	UNKNOWN	**Impaired (very slow motion)**	**Impaired (very slow motion)**	**Impaired (very slow motion)**
Motion perception – basic (coherence)[63]	Normal	Normal	UNKNOWN	**Impaired (very fast motion)**	**Impaired (medium to very fast motion)**	UNKNOWN
Motion perception – structure (SFM)[63]	Normal	Normal	UNKNOWN	**Impaired**	**Impaired**	**Impaired**
Motion perception – **biological** unmasked PLDs (Exp. 1)	Normal	Normal	Normal	Normal	Normal	Normal
Motion perception – **biological** perceptual thresholds (Exp. 1)	Normal	Normal	Normal	Normal	Normal	Normal
Motion perception – **biological** unmasked PLDs (Exp. 2)	Normal	Normal	Normal	Normal	Normal	Normal
Motion perception – **biological** perceptual thresholds (Exp. 2)	Norman	Normal	Normal	Normal	Normal	Normal

Table 2

Experiment 1: Biological motion perceptual thresholds of patients and controls. Thresholds indicate the number of noise points masking the stimuli while performance is at 82% accuracy (see Methods). Statistical values (t and p values) represent single-case versus control group comparisons (41). Ventral visual patients' perceptual thresholds for biological motion were not significantly different from those of three control groups: healthy age-matched (group 1), brain-damaged (group 3), and younger controls (group 2, see Results). Importantly, the group of ventral patients performed significantly better than the group of patients with lesions to pSTS or vPMC (see Results).

* At the upper end of the controls' distribution, i.e. performing better than the average.

Patient		Vs. healthy age-matched controls (control group 1)			Vs. brain-damaged controls (control group 3)									
					All (n=54)		LH damage only (n=43)		RH damage only (n=11)		With "critical" pSTS lesion (n=9)		With "critical" vPMC lesion (n=10)	
	Thres-hold	Mean threshold ± S.D.	t	p	t	p	t	p	t	p	t	p	t	p
EL	18.38	19.15 ± 8.74	-0.086	0.933	1.47	0.15*	1.5	0.14*	1.29	0.22*	4.187	0.002*	3.66	0.003*
GB	18.73	19.15 ± 8.74	-0.047	0.963	1.54	0.13*	1.57	0.12*	1.35	0.20*	4.319	0.002*	3.78	0.003*
SH	11.33	19.15 ± 8.74	-0.866	0.401	0.12	0.90	0.09	0.93	0.22	0.83	1.528	0.082*	1.27	0.117*
CR	13.97	28.66 ± 7.91	-1.8	0.09	0.63	0.53	0.62	0.53	0.62	0.54	2.52	0.018*	2.17	0.03*
SM	12.25	25.06 ± 7.54	-1.64	0.12	0.3	0.77	0.27	0.78	0.36	0.72	1.875	0.049*	1.58	0.07*
EC	9.57	20.08 ± 7.87	-1.29	0.22	-0.21	0.83	-0.26	0.79	-0.047	0.96	0.864	0.206*	0.676	0.26*

Table 3

Summary of patients' lesions. The lesion size is based on the results of the lesion delineating procedure (see also Supplementary Material). Due to the low spatial coverage of GB's, SH's and EC's clinical scans, their lesion size reflects a spatial interpolation across the lesion locations in the clinical images that were available. The assessment of the overlap of the lesion with regions associated with biological motion processing is predominantly based on a recent meta-analysis ((13), see text for details), as demonstrated in Figure 2. Overlap with MT+/V5 is based on SM's functional localization, and on MT+/V5 reported location for the other patients ((83), see Experimental Procedures). Overlap scale relates to foci reported in the meta-analysis with $Z >= 3.2$ score (equivalent to p<=0.0005). Overlap notations: No – none, hardly ~ <10%, mildly ~ 10-20%, partially ~ 20-60%, mostly > 60 -70%, all – 100%. EBA partitions: v-EBA – aspect of EBA ventral to MT/V5, mt-EBA – aspect of EBA overlapping MT/V5, a-EBA – aspect of EBA anterior to MT/V5 (47, 48).
* GB's, CR's, and EC's lesion sizes were approximated on an MNI template brain and therefore provided in MNI normalized space units (mm^3) which might be an overestimation relative to native space volume (84).

		EL	GB	SH	CR	SM	EC
Lesioned hemisphere		Left	Left	Left	Right (+ left)	Right	Right
Lesion extent		Extensive	Extensive	Extensive	Intermediate	Small	Extensive
Lesion approximate size in native* space (mm^3)		43028	49929*	31751*	1510	952	62959*
Lesion overlap: ventral surface	Regions sensitive to human movements	No	**Mostly**	**All**	No	Hardly	**Mostly**
	Regions sensitive to static bodies	No	**All**	**All**	No	**Partially**	**All**
	Regions activated to body movement	No	**All**	**All**	No	Hardly	**Mostly**
Lesion overlap: lateral occipito-temporal surface	Regions sensitive to human movements	**Partially**	Hardly	No	No	No	Mildly
	Regions sensitive to static bodies	**Partially**	No	No	No	No	Mildly
	regions activated to body movement	**Partially**	No	No	No	No	Hardly
	MT+/V5	**Partially**	No	No	No	No	**Partially (?)**
EBA partitions	v-EBA	No	**Partially**	No	No	**Mostly**	**All**
	mt-EBA	**Partially**	Hardly	No	No	No	Hardly
	a-EBA	Mildly	No	No	No	No	**Partially**
Other	pSTS	Mildly	No	No	No	No	No
	vPMC	No	No	No	No	No	No
	Parietal	No	No	No	No	No	No

FIGURES

Figure 1

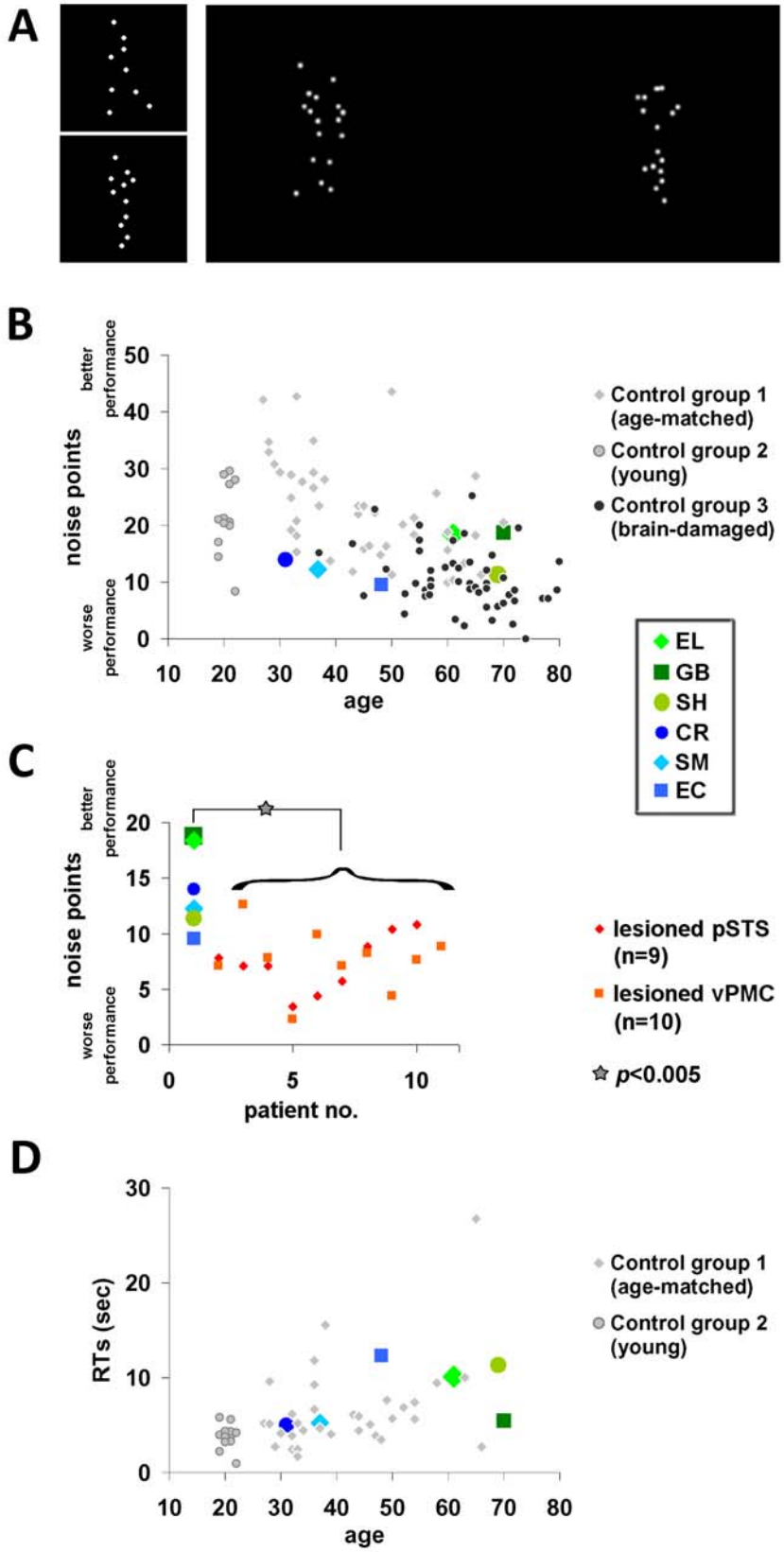

Biological motion perception: Experiment 1 paradigm and results. (A) Left - static snapshots from the unmasked point light displays (PLDs) presented in the action recognition phase; participants were required to verbally describe them. Right - to determine perceptual thresholds, two masked PLDs embedded in noise points were presented simultaneously, one on the right and one on the left, one containing a biological movement (here on the left), and the other a spatially scrambled version of that movement. The task was to determine which side contained the moving human figure. The noise points were added adaptively according to individual performance (see Methods). (B) Individual perceptual thresholds (y axis) of the ventral visual patients and the three control groups against age (x axis). Perceptual thresholds represent the number of noise points that can be tolerated while performing at 82% accuracy (more noise points correspond to better performance). Each ventral patient was not significantly different from any of the control groups, and performed similarly or better than the brain damaged controls with spared ventral cortex (11) (see Table 2). (C) Ventral visual patients' performance was significantly better than that of brain-damaged controls (11) whose lesions invaded regions critical for biological motion perception (pSTS, vPMC). (D) Response times (y axis) as recorded during the experiment plotted against age (x axis). RTs are not very informative as instructions did not require speeded responses (participants were able to respond leisurely and take breaks). Response times of the brain damaged control group were not available. Ventral visual patients' response times (apart from EC, see Results) were not significantly slower than their age-matched controls.

Figure 2

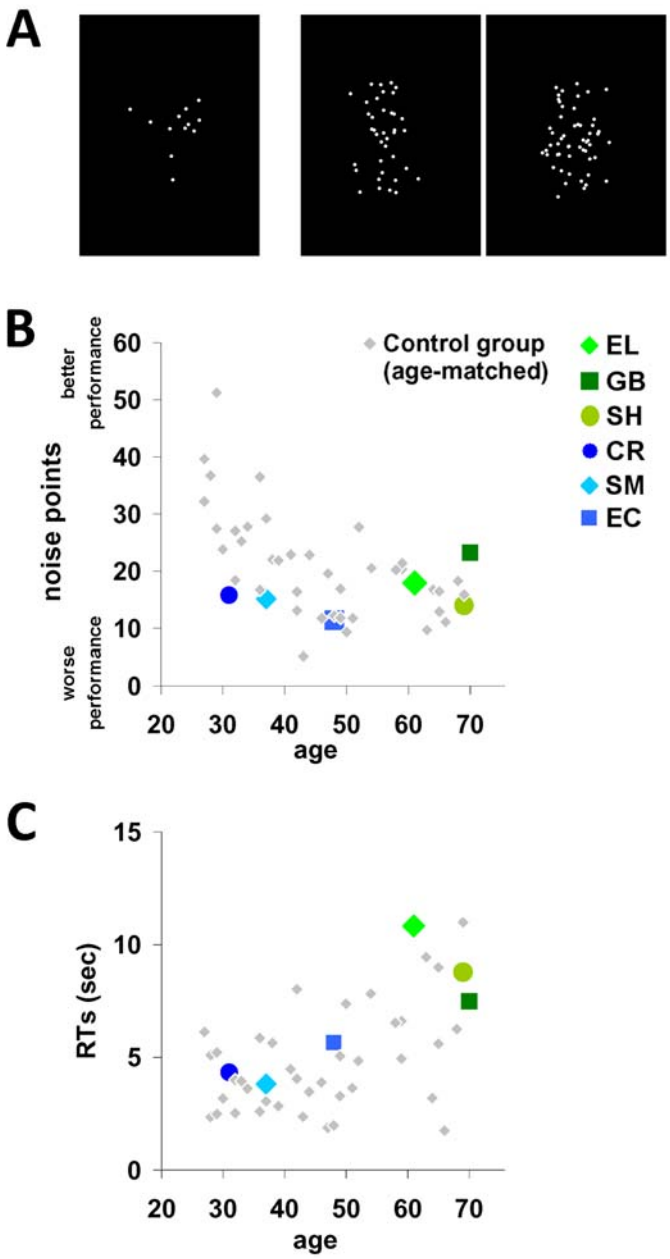

Biological motion perception: Experiment 2 paradigm and results. (A) Left - static unmasked PLD snapshot presented in the action recognition phase, participants were required to verbally describe them. Middle and right - to determine perceptual thresholds, each trial presented a masked PLD either containing a biologically moving figure (middle) or a spatially scrambled version of it (right), and the task was to determine whether a moving figure was embedded in the display. The noise points were added adaptively according to individual performance with 75% accuracy (see Methods). (B) Individual perceptual thresholds (y axis) of the ventral visual patients and the age-matched controls against age (x axis). Perceptual thresholds determined similar to Figure 1 (see Methods). Although patients commonly perform more poorly than healthy matched controls, the performance of each ventral patient was not significantly different from that of their healthy age-matched controls (see Results).

(C) RTs are not very informative as instructions did not require speeded responses (participants were able to respond leisurely and take breaks). Ventral visual patients' response times were not significantly slower than their age-matched controls (see Results).

Figure 3

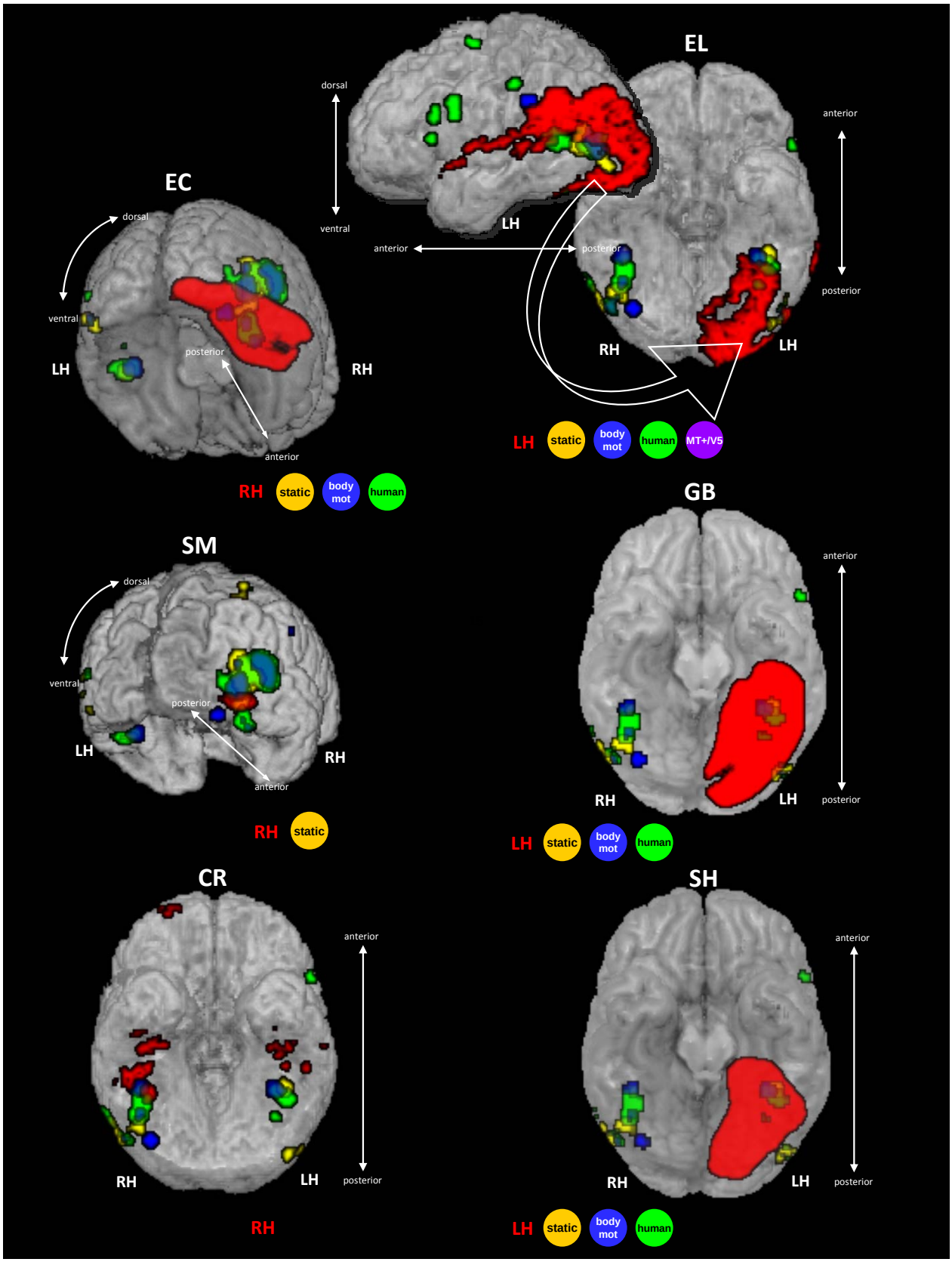
EL
dorsal
ventral
anterior
posterior
LH
RH
LH
EC
dorsal
ventral
posterior
anterior
LH
RH
RH
static
body mot
human
LH
static
body mot
human
MT+/V5
SM
dorsal
ventral
posterior
anterior
LH
RH
RH
static
GB
anterior
posterior
RH
LH
LH
static
body mot
human
CR
anterior
posterior
RH
LH
RH
SH
anterior
posterior
RH
LH
LH
static
body mot
human

Situating the patients' lesions with respect to visual regions standardly associated with biological motion processing, presented in rendered fashion. Lesion of each patient is delineated in red based on the structural images (see Methods and Supp. Mat.). Regions consistently associated with biological motion processing are based on statistical maps of a meta-analysis (13): regions in blue are significantly activated to biological motion, regions in yellow are sensitive to static bodies, regions in green are sensitive to human movement over non-human movements. As summarized in Table 3, ventral visual regions associated with all the three types of biological motion perception were severely affected by brain damage in one or more of the ventral visual patients, including the ventral aspect of extrastriate body area (v-EBA, in EC, SM, GB). This indicates that the spared perceptual thresholds for biological motion perception do not rely on the integrity of the ventral visual regions associated with biological motion processing. MT+/V5 – middle temporal motion sensitive region, RH/LH – right/left hemisphere. See also Table 3.

Figure 4

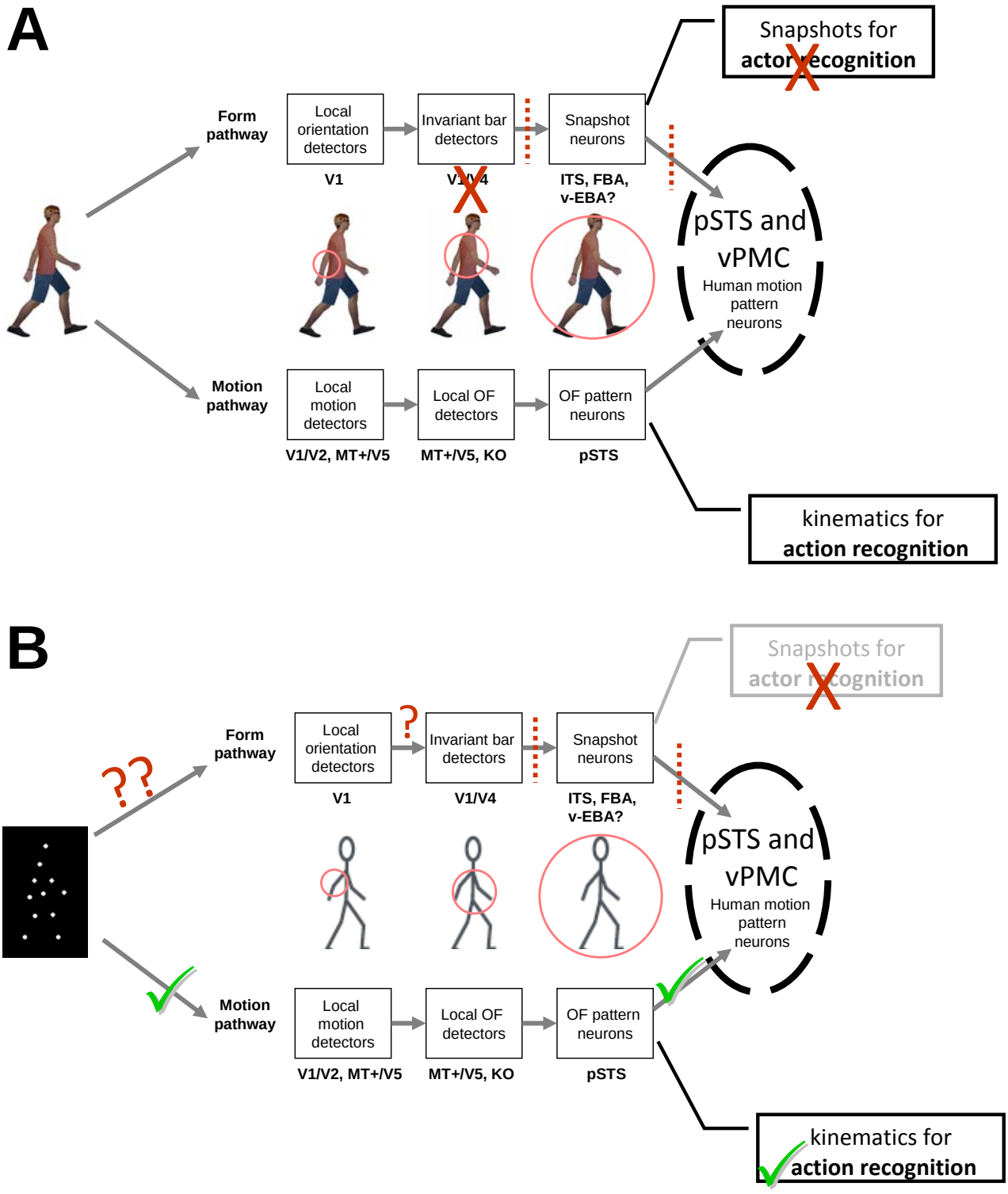

Adaptation of the model for biological motion recognition based on Giese & Poggio (52). (A) The original model by Giese & Poggio with proposed distinctions: the form pathway's main role involves snapshots for actor recognition, while the motion pathway's main role involves kinematic patterns for human movement recognition. Brick color indicates how brain damage to ventral cortex predominantly affects the form processing pathway that is involved in snapshot creation, thereby impairing

actor but not action recognition. (B) Adaptation of the model to PLDs. Information flow in the case of PLDs resembles that of damaged ventral visual cortex (A), as the information processed by the form pathway is insufficient, leading to abnormal actor recognition. At the same time, the information processed by the motion pathway is not significantly affected, so that the movement can be recognized. Based on our results, we speculate that the perception of human movement can be achieved based on motion kinematics alone. OF – optic flow, V1/V2/V4 – visual retinotopic regions, FBA – fusiform body area, v-EBA – ventral aspect of extrastriate body area, ITS – inferior temporal sulcus, pSTS- posterior superior temporal sulcus, vPMC – ventral premotor cortex, MT+/V5 – middle temporal motion-sensitive regions, KO – kinetic occipital.

Supplementary Material

Case descriptions: Additional details

Left hemisphere lesions

EL case description

EL suffered a left posterior cerebral artery infarct affecting the medial temporal lobe and occipital lobe as revealed by a 3T MRI scan (see Figure 3). EL has participated in many previous studies, which provide detailed description of her abilities and impairments (1-7). Briefly, these earlier studies revealed that she has pure alexia as well as some difficulty in object and face recognition. She worked as a reading specialist prior to her stroke.

GB case description

GB suffered a posterior cerebral artery (PCA) stroke. An MRI scan performed 3 years post-stroke revealed a lesion affecting two thirds of the left temporal lobe and the inferior aspect of the left occipital lobe (see Figure 3). She suffers from pure alexia and, as uncovered in previous studies (5-7), she has some mild impairment in object and face recognition, too. GB worked as a graphic artist prior to her stroke.

SH case description

SH suffered from a lesion affecting left temporo-occipital structures and the left thalamus, compatible with a left PCA infarct (see Figure 3). He suffers from pure alexia, and, as uncovered in previous studies (6, 7), he has mild impairments in face and object recognition. SH worked as a lawyer prior to his stroke.

Right hemisphere lesions

SM case description

SM sustained a closed head injury in a motor vehicle accident at the age of 18 and recovered well after rehabilitation, aside from a persisting visual agnosia and prosopagnosia. Recent neuroimaging (8) revealed a circumscribed lesion in the posterior portion of the right lateral fusiform gyrus. Further details of his medical and neuropsychological history can be found in previous studies (5, 6, 9-12). SM works in a photography studio.

CR case description

CR suffered from a right temporal lobe abscess with a complicated medical course including a history of Group A toxic shock syndrome, pneumonia, cardiac arrest, candida bacteremia, and metabolic encephalopathy in May 1996, approximately 15 years prior to his participation in this study. MR scans reveal a right temporal lobe lesion consistent with acute micro-abscesses of the right temporal lobe and medial occipital lobe and there are small lacunae in the left hemisphere, as well. CR has participated in several previous studies (5, 6, 9, 10, 13) that highlight his visual perceptual deficits which include impaired recognition of objects and of faces. CR completed community college and now runs a restaurant.

EC case description

EC was tested four years after suffering an infarction. The radiology report states that there is low attenuation at the right temporal lobe and right occipital lobe posteriorly,

consistent with a right PCA infarct. She showed difficulties in both face and object recognition on screening tests conducted prior to these experiments (5).

Additional experimental details

Experiment 1: Additional experimental details

This experiment has been described in detail elsewhere (14, 15). Biological motion animations were created by videotaping an actor performing various activities, and encoding only the joint positions in digitized videos (16). In the videos, the joints were represented by 12 small white points against a black background (Figure 1A; for an animated example, see Supplementary Figures S2-S3).

Each animation consisted of 20 distinct frames and was displayed for 0.5 s (16.5 ms interframe interval, 60 Hz). The final frame then remained visible for 0.3 s, after which the animation looped from the beginning. Since a joint could become occluded by other body parts during an action, some points were briefly invisible at times.
For each of the animations, the matched spatially-scrambled animation was created by scrambling the starting positions of the 12 points while keeping the motion trajectories of each point unchanged. The starting positions of the scrambled points were chosen randomly within a region so that the total area encompassed by the scrambled animation was similar to that of the original non-scrambled biological animation (see Figure 1A).

Experiment 2: Additional experimental details

Stimuli

This experiment included the seven animations from Experiment 1 and five additional ones (climbing stairs, skipping rope, kicking leftward with right leg, bending down, and pitching). All the animations were created in the same manner as described in Experiment 1. For each animation, a spatially scrambled matched version animation was created as described in Experiment 1. As in Experiment 1, a variable number of noise points, each with a motion trajectory as one of the points from the target biological motion animation were also presented on each trial of the perceptual threshold assessment (in each trial, all the noise points motion trajectories were from the same animation), and the initial spatial location of the noise points was determined randomly.

The point-light display that was presented centrally in each trial subtended approximately 4 x 8 degrees visual angle when viewed from 55 cm while the region populated by the point-light display and the noise points together was approximately 8 x 12 degrees visual angle. On each trial, the target (or non-target) point-light display was presented at a randomly jittered location within a 2.2° radius from the centre of the screen. Stimuli were presented and responses recorded using Matlab (Mathworks, Natick, MA, USA) and the Psychophysics Toolbox V2.54 (17, 18).

Procedure

The experiment started with assessing action recognition of unmasked point light display animations. The participants were not informed about what they were about to view and were instructed to describe what they saw. Following this phase we assessed perceptual thresholds. Each participant completed a practice block that included 16 trials with a range of predetermined number of noise points (ranging from 0 to 40). The practice was followed by the main experimental block, which included 60 trials in which the number of noise points was determined in an adaptive manner,

contingent on performance, beginning with 10 noise points. Varying the number of noise points enabled us to measure biological motion detection thresholds at which each participant performed at 75% accuracy (19), and this was done using the same Bayesian adaptive paradigm as in Experiment 1 (QUEST). The task became more difficult with increasing number of noise points.

Each trial started with a white fixation cross displayed at the centre of the screen for 750 ms, after which the point-light displays were presented along with noise points. The animations were repeated continuously until a response was given. After each response, a visual feedback cue appeared for 750 ms (green fixation cross for correct, red for incorrect).

Data Analysis

Thresholds were calculated for each patient and for each of the control participants, and data (thresholds and RTs) were analyzed as in Experiment 1.

Ventral visual patients' structural image acquisition

EL

EL's anatomical MR scans were acquired at the Brain Imaging Research Center (BIRC) Pittsburgh on a Siemens Allegra MRI 3T scanner using a head coil, when she was 60 y.o., approximately one year prior to her participation in this study and 14 years after her injury. The scan acquired 192 MPRAGE sagittal slices (1mm thickness, inplane resolution of 1x1 mm^2, matrix = 256x256, repetition time 1740ms, echo time 3.04ms, inversion time 1000ms, flip angle =8°).

GB

GB's MR clinical structural scans were acquired on a 1.5 T GE Genesis Signa MR scanner equipped with a head coil, approximately 3 years prior to her participation in this study. These included 23 axial T2 images (slice thickness = 5.5mm, 7mm gap, image size 512x512, pixel spacing 0.42968 x 0.42968 mm^2, echo time = 96.512 ms, no. of averages = 2, flip angle =90°).

SH

SH's CT clinical structural scans were acquired on a Siemens SOMATOM Sensation 4 CT scanner when he was 63 y.o., and approximately 6 years prior to his participation in this study. These included axial images with slice thickness/overlap of 5.0/2.5mm.

SM

SM's MRI structural scans were acquired with identical parameters to those of EL's (see above) at the Brain Imaging Research Center (BIRC) Pittsburgh when he was 35 y.o. This was 17 years after his injury and approximately 2 years prior to his participation in this study (for details, see (8)).

CR

CR's MRI structural scans were acquired at the Magnetic Resonance Research Center, University of Pittsburgh Medical Center on a 1.5 T Signa whole body scanner (General Electric Medical Systems, Milwaukee, WI), approximately 3 years after he had metabolic encephalopathy and approximately 12 years prior to his participation in

this study. This included 124 slices of 1.5mm thickness with an inplane resolution of 0.9375x0.9375 mm^2, matrix of 256x256.

EC

EC's CT clinical structural scans were acquired on a GE Medial Systems LightSpeed QX/i CT scanner when she was 40 y.o., and approximately 8 years prior to her participation in this study. These included 34 axial images without contrast with slice thickness of 2.5mm (through the posterior fossa) and 7.5mm (from the posterior fossa to the vertex), 512x512 image size, and pixel spacing of 0.449219x0.449219 mm^2.

Lesion tracing criteria

We used an established procedure and most of these details are published elsewhere (5). We describe below specific modifications we made to document the lesion of each patient, where necessary.

EL: Since the average intensity values varied across each structural image regardless of the lesion (e.g. between anterior and posterior regions, or right and left hemispheres), the definition of the lesioned tissue was not based solely on absolute intensity values and relative local differences were considered, as well. Instead, the definition of the lesioned tissue also took into account abrupt local changes in intensities between lesioned and adjacent healthy tissue, and continuity of abnormal lesioned tissue. Locally, lesioned tissue always had substantially lower values of intensity than healthy tissue. In most parts of EL's brain and around the lesion, healthy tissue intensity values ranged from 200 to above 350, while lesioned tissue intensity values ranged from 54 to 170. However, in specific locations, the value, 170,

was considered healthy tissue (adjacent to value of 117 of a lesioned tissue). We provide lesion size estimates based on local intensity variations and continuity assessment, and also a more conservative estimation based on intensity values <150 in the predefined lesion zone (see Table 3).

SM: SM's structural images also revealed local variations in intensity values; thus, as with EL, we delineated the lesion based on intensity values, continuity of the lesioned tissue, and abrupt changes in local intensity values between the lesion and adjacent healthy tissue. Common values for healthy tissue were above 200 to even above 350, however, locally healthy tissue could have value of 171. Lesioned tissue typically had values ranging from as low as 60's to values around 150, however, locally, values of 160 or 174 could be attributed to lesioned tissue. We provide the lesion size estimate according to the criteria laid out above, along a conservative estimate for lesion when lesioned intensities < 160.

CR: Because CR's lesion is of a different etiology than that of EL and SM, the lesion delineation criteria were different. CR has a definitive lesion in the right temporal lobe (see above) that is evident and confirmed by an expert neuroradiologist in the past and during the current study. In addition, there are foci of petechial hemorrhage seen along the grey/white junction at multiple areas that appear as a very dark centre (intensity values of below 35) bordered by very bright intensity tissue (intensity above 120). Healthy tissue in CR's structural images had intensity values of 55-95. There are, however, some small foci of enhancement in the left hemisphere (perhaps resolved abscesses) and so we adopt a conservative approach here and leave open the possibility of additional left hemisphere insult.

Lesioned tissue in GB's, EC's, and SH's original clinical structural images were used to guide delineation in a normalized MNI canonical brain. GB's original DICOM images were loaded into MATLAB (Mathworks, Natick, MA, USA) where intensity values of lesioned tissue were above 0.5, while healthy tissue intensity values were below 0.4. Due to technical issues with MATLAB reading EC's DICOM images, EC's structural images were loaded into MicroDicom (http://www.microdicom.com/) and then exported to bitmap images. Typically lesioned tissue intensity values were below 105, while healthy tissue values were above 110. In the lesion delineation process we also took into account (as with the other patients) continuity of the lesioned tissue, and abrupt intensity changes between the lesion and adjacent healthy tissue. After the lesion tracing in the original images detailed above, an approximated corresponding delineation was carries out onto a single subject T1 SPM MNI-normalized template. Following that, we manually interpolated each lesion into a continuous lesion in a conservative manner. This was achieved in MRIcroN software (www.mrico.com) where the originally traced lesioned volume (in axial sections), was then filled in manually in the orthogonal section planes (sagittal and coronal) by linear interpolation (see Supp. Fig. S4).

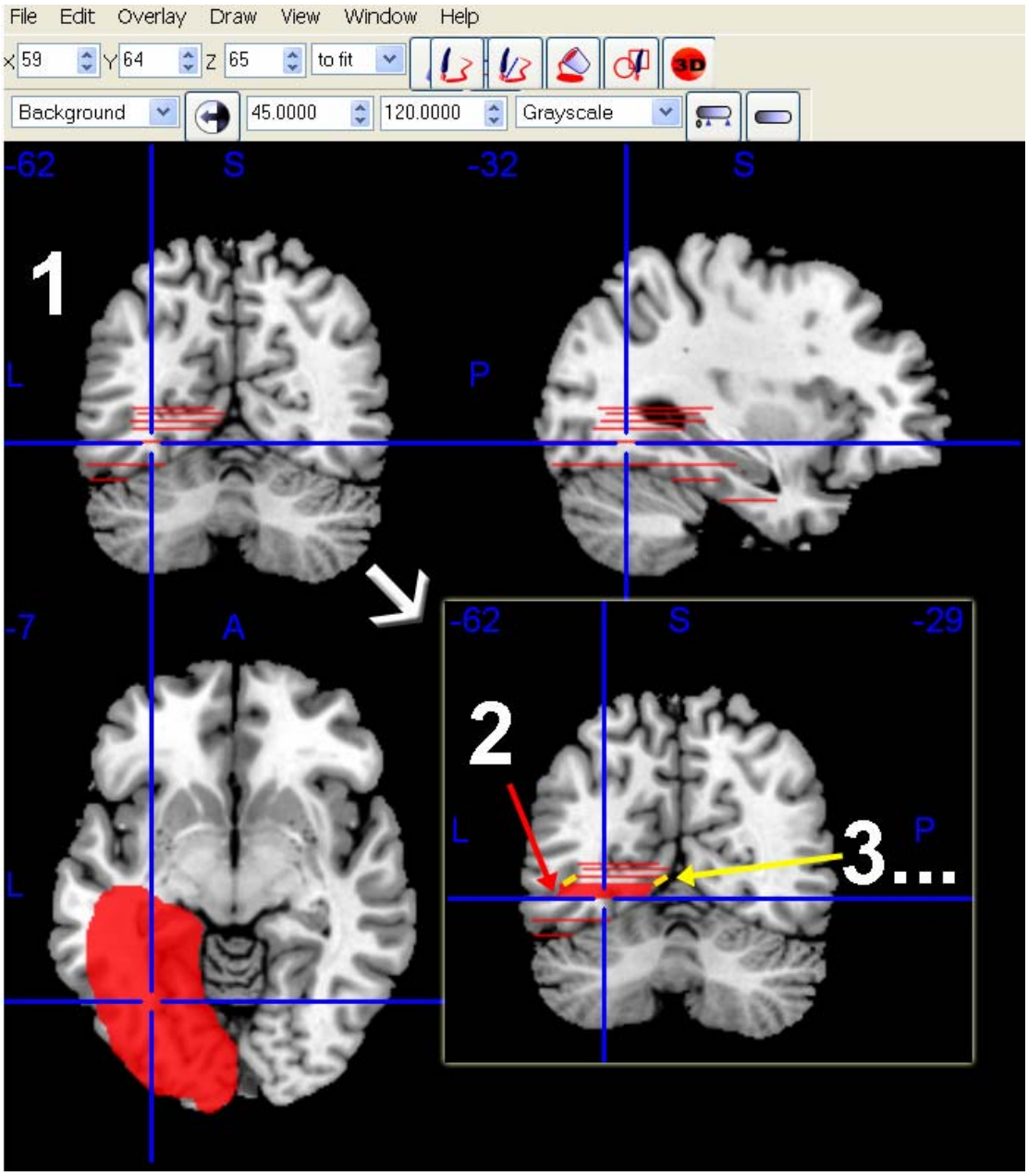

Supplementary Figure S4. Demonstrating the filling-in procedure of the traced lesion volume (as was done in the case of GB, EC, and SH). The filling in was achieved by linearly interpolating in the coronal and sagittal planes between the traces of the lesion (in the axial planes, see above bottom left). One step is shown (in a coronal section) where the interpolation is performed between two traced axial slices (1), and filled in red (2). The step to follow repeats this procedure by filling in the region enclosed by the yellow and red lines (3).

Supplementary Table S5– Exp 2 statistical results

Experiment 2: biological motion perceptual thresholds of patients are not significantly different from their age-matched healthy controls. Thresholds indicate the number of noise points masking the stimuli while performance is at 75% accuracy (see Methods). Significance values as in Table 2.

Patient	Vs. healthy age-matched controls	
	T	P
EL	0.45	0.66*
GB	1.3	0.22*
SH	-0.19	0.85
CR	-1.41	0.18
SM	-0.95	0.36
EC	-0.74	0.48

Supplementary references

1. McKeeff TJ & Behrmann M (2004) Pure alexia and covert reading: Evidence from Stroop tasks. *Cogn Neuropsychol* 21(2):443-458.
2. Mycroft RH, Behrmann M, & Kay J (2009) Visuoperceptual deficits in letter-by-letter reading? *Neuropsychologia* 47(7):1733-1744.
3. Montant M & Behrmann M (2001) Phonological activation in pure alexia. *Cogn Neuropsychol* 18(8):697-727.
4. Behrmann M, Nelson J, & Sekuler EB (1998) Visual complexity in letter-by-letter reading: "Pure" alexia is not pure. *Neuropsychologia* 36(11):1115-1132.
5. Gilaie-Dotan S, *et al.* (2013) The role of human ventral visual cortex in motion perception. *Brain* 136(Pt 9):2784-2798.
6. Behrmann M & Plaut DC (2014) Bilateral Hemispheric Processing of Words and Faces: Evidence from Word Impairments in Prosopagnosia and Face Impairments in Pure Alexia. *Cereb Cortex* 24(4):1102-1118.
7. Habekost T, Petersen A, Behrmann M, & Starrfelt R (2014) From word superiority to word inferiority: Visual processing of letters and words in pure alexia. *Cogn Neuropsychol*:1-24.
8. Konen CS, Behrmann M, Nishimura M, & Kastner S (2011) The functional neuroanatomy of object agnosia: a case study. *Neuron* 71(1):49-60.
9. Gauthier I, Behrmann M, & Tarr MJ (1999) Can face recognition really be dissociated from object recognition? *J. Cogn. Neurosci.* 11(4):349-370.
10. Marotta JJ, Genovese CR, & Behrmann M (2001) A functional MRI study of face recognition in patients with prosopagnosia. *Neuroreport* 12(8):1581-1587.
11. Behrmann M & Kimchi R (2003) What does visual agnosia tell us about perceptual organization and its relationship to object perception? *J Exp Psychol Hum Percept Perform* 29(1):19-42.
12. Nishimura M, Scherf S, & Behrmann M (2009) Development of object recognition in humans. *F1000 biology reports* 1:56.
13. Behrmann M & Williams P (2007) Impairments in part-whole representations of objects in two cases of integrative visual agnosia. *Cogn Neuropsychol* 24(7):701-730.
14. Gilaie-Dotan S, Bentin S, Harel M, Rees G, & Saygin AP (2011) Normal form from biological motion despite impaired ventral stream function. *Neuropsychologia* 49(5):1033-1043.
15. Saygin AP (2007) Superior temporal and premotor brain areas necessary for biological motion perception. *Brain* 130(Pt 9):2452-2461.
16. Ahlstrom V, Blake R, & Ahlstrom U (1997) Perception of biological motion. *Perception* 26(12):1539-1548.
17. Brainard DH (1997) The Psychophysics Toolbox. *Spat Vis* 10(4):433-436.
18. Pelli DG (1997) The VideoToolbox software for visual psychophysics: transforming numbers into movies. *Spat Vis* 10(4):437-442.
19. Watson AB & Pelli DG (1983) QUEST: a Bayesian adaptive psychometric method. *Percept Psychophys* 33(2):113-120.